Spring 5-3-2011

Particle to Gas Heat Transfer in a Circulating Fluidized Bed Riser

Yassir Makkawi
Heriot-Watt University

PARTICLE TO GAS HEAT TRANSFER IN A CIRCULATING FLUIDIZED BED (CFB) RISER

Yassir T. Makkawi
European Bioenergy Research Institute (EBRI), School of Engineering and Applied Science, Aston University, Birmingham B4 7ET, United Kingdom
T: +44 (0)121 204 3398; E: y.makkawi@aston.ac.uk

ABSTRACT

The main objective of this study was to measure the heat transfer from particle to gas in a dilute CFB riser ($\varepsilon > 0.8$) and to derive a predictive equation for the local particle-gas heat transfer coefficient. This coefficient was found to be a strong function of the particle velocity, concentration and length of the heat transfer section. Accordingly, a new correlation in terms of these parameters is proposed.

INTRODUCTION

Studies on heat transfer in a Circulating Fluidized Bed (CFB) have been mainly focused on two characteristic heat exchange mechanisms (i) exchange between the wall to gas or particle (ii) exchange between the gas to particle. While considerable amount of research has been conducted on the first mechanism, which is relevant to fluidized bed boilers, limited attention has been paid to the second mechanism. Particle to gas heat transfer is of particular interest in CFB thermo-chemical processes, such as biomass thermal conversion and the new emerging technology of chemical looping. In biomass gasification/pyrolysis, circulating hot particles, such as sand and char, are used to drive the thermochemical conversion of fresh biomass feed via particle-gas heat exchange. While in chemical looping, hot metal particles are circulated between two reactors as a mean for carrying oxygen. This process is also relevant to drying and catalytic reactions.

MOTIVATION OF THIS STUDY

Review of the published literature on heat transfer in dilute-phase suspension, such as in a CFB riser, indicate considerable uncertainties with respect to heat transfer coefficient. Table 1 shows two of the most widely used correlations and two recently developed ones. The literature contain a fairly large number of studies, using the correlations of Ranz and Marshall (1) and Gunn (2), in the simulation of particle-gas heat transfer in a CFB, e.g. Xie et al. (3) and Watanabe and Otaka (4).

We recently carried out a numerical simulation, *Fluent* code (5), to investigate the particle-gas heat transfer in dense suspension (bubbling bed) and dilute suspension (CFB riser). Using Gunn's correlation, the latter case has shown poor agreement with experimental measurements, while excellent agreement has been noticed for the case of dense suspension as shown in Fig. 1. The same was observed when applying Ranz

and Marshall correlation (1). It should be noted that, in both cases, the hydrodynamics were in good agreement with the experimental measurement (not shown here).

Table 1. Particle-gas heat transfer correlations

	Correlation	Author	Range
(a)	$Nu = 2 + 0.6\,\mathrm{Re}_p^{0.5}\,\mathrm{Pr}^{0.33}$	Ranz & Marshall (1)	$10 < \mathrm{Re} < 10^4$, $\mathrm{Pr} > 0.7$
(b)	$Nu = \left(7 - 10\varepsilon + 5\varepsilon^2\right)\left(1 + 0.7\,\mathrm{Re}_p^{0.2}\,\mathrm{Pr}^{0.33}\right) + \left(1.33 - 2.4\varepsilon + 1.2\varepsilon^2\right)\mathrm{Re}_p^{0.7}\,\mathrm{Pr}^{0.33}$	Gunn (2)	$0.3 < \varepsilon < 1.0$
(c)	$Nu = 8.295\times10^{-7}\,\mathrm{Re}_p^{\,5.3365}\,F_m^{-1.3863}Fe^{-5.0530}$	Rajan et al. (6)	dilute phase
(d)	$Nu = 1.336\times10^{-4}\,\mathrm{Re}_p^{\,2.7624}\,F_m^{0.6792}Fe^{-1.8344}$	Rajan et al. (6)	dense phase

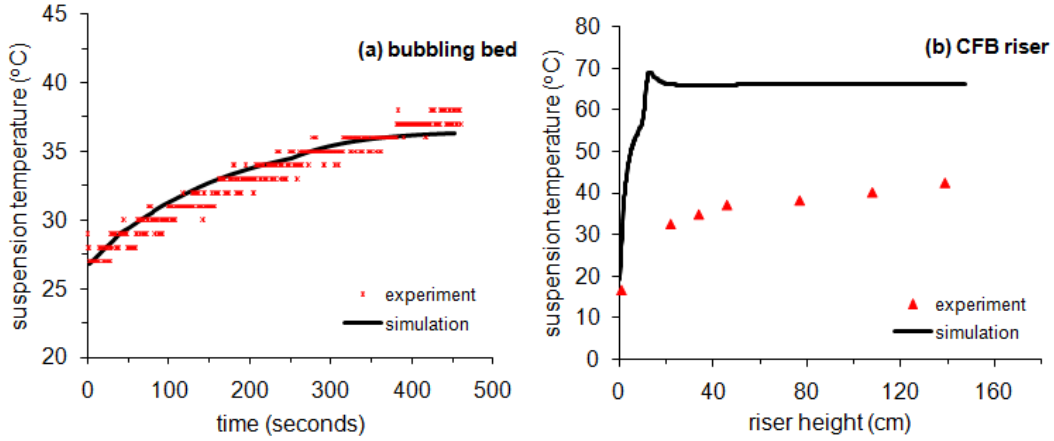

Figure 1. Simulation and experiment results of suspension temperature in (a) bubbling bed with initial cold bed fluidized by hot air and (b) CFB with hot particles inlet and cold fluidizing air.

Rajan et al. (6) recently developed a new correlations for particle-gas heat transfer coefficient in a vertical pneumatic conveyer operating at low particle to gas flow ratio in the range of $F_m < 1.0$. The reported correlations, given in Eq. (c) and Eq. (d) in Table 1, were derived from data collected at the inlet and exit of the conveyers, thus representing the overall average performance across the whole conveyer height. The coefficients were categorized to dilute and dense flow regimes, however the authors did not give clear cut boundaries between what they call “dense” and “dilute”.

In this study, the main objective was to carry out localized measurements in a CFB riser operated at low suspension density within the range of $\varepsilon > 0.8$, this corresponds to a particle-gas flow ratios of $0.5 < F_m < 10$. The data was then used to derive a simple correlation for particle-gas heat transfer coefficient.

EXPERIMENTAL

Set-up and Procedure

Fig. 2 shows a schematic diagram of the circulating fluidized bed, which mainly comprises a 163 cm height and 5.2 cm diameter riser, connected to a primary and secondary cyclones and a particle feeding/receiving tank. The fluidizing air flow rate was measured by two rotameter, giving a maximum flow rate of 1300 lit/min. The average suspension temperature and pressure along the riser were measured by eight thermocouples and pressure transducers. Two electric heating elements, wrapped around the particle feeding tank, were used for heating the particles up to a maximum temperature of 100 ºC. The riser, downer and particle tank were all thermally insulated to minimize heat losses. Glass beads and sand in the range of 235 μm to 700μm were used as the bed material. The experiment starts by loading the feeding tank with around 10 kgs of particles. The particles are then heated to the desired temperature using the electric heater at a selected set point. At fluidization, the pressure and temperature of the suspension along the riser were logged at the rate of 1 Hz. The particle mass flow rate was determined by relating the particle mass to collecting time. To ensure comprehensive data, a total of 48 different combinations of operating conditions were considered.

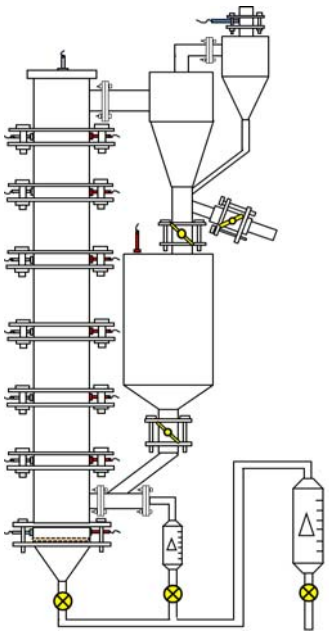

Figure 2. Circulating fluidized bed

Data Analysis Method

If we assume uniform cross-sectional particle and gas distribution and negligible downfall of particles at the wall, then local heat transfer coefficients along the riser can be estimated by dividing the riser to a number of axial segments. Fig. 3 shows a schematic representation of this method. The heat transfer in each section was calculated using the measured gas/particle flow rate and temperatures at the end of each section such that:

$$q = m_g C_{p,g}(T_{g,i+1} - T_{g,i}) = m_s C_{p,s}(T_{s,i+1} - T_{s,i}) \quad (1)$$

The average void fraction (ε) for each bed section of length (z) was determined from pressure drop measurement (ΔP) such that,

$$\varepsilon = 1 - \frac{\Delta P}{(\rho_s - \rho_g) g z} \quad (2)$$

With the available information on temperature and pressure variations along various sections of the riser, the local particle-gas heat transfer coefficient was determined by relating the localized heat transfer (q) to the particle surface area (A_s) and the temperature difference between the two phases (ΔT) as follows:

$$h = \frac{q}{A_s \Delta T} \quad (3)$$

The particles surface area was related to the estimated void fraction, such that,

$$A_s = \frac{6(1-\varepsilon)}{d_s} A_c z \quad (4)$$

where A_c is the riser cross-sectional area and d_s is the particle diameter. The heat transfer driving force (ΔT) was given in terms of the log mean temperature as follows:

$$\Delta T = \frac{(T_{g,i} - T_{s,i}) - (T_{g,i+1} - T_{s,i+1})}{\log[(T_{g,i} - T_{s,i}) / (T_{g,i+1} - T_{s,i+1})]} \quad (5)$$

In obtaining the particle temperature, we start by assuming that the measured temperature along the riser represents the suspension temperature or bed temperature (gas and particle mixture). Hence, this can be expressed as volume-weighted average temperature:

$$T_{mix} = (1-\varepsilon)T_s + \varepsilon T_g \quad (6)$$

The exit air temperature in each section is obtained from Eq. 6 as follows:

$$T_{g,i+1} = \frac{T_{mix,i+1} - (1-\varepsilon_{i+1})T_{s,i+1}}{(1-\varepsilon_{i+1})} \quad (7)$$

Equating both sides of Eq. 1, the exit particle temperature in each section is given by:

$$T_{s,i+1} = T_{s,i} - \frac{m_g C_{p,s}}{m_s C_{p,g}} (T_{g,i+1} - T_{g,i}) \quad (8)$$

Taking $\alpha = m_g C_{p,g} / m_g C_{p,g}$, and substituting Eq. 7 into Eq. 8, gives

$$T_{s,i+1} = \frac{1}{\varepsilon_i + \alpha(1-\varepsilon_i)} \left[T_{s,i}\varepsilon_i - \alpha(T_{mix,i+1} - T_{g,i}\varepsilon_i) \right] \quad (9)$$

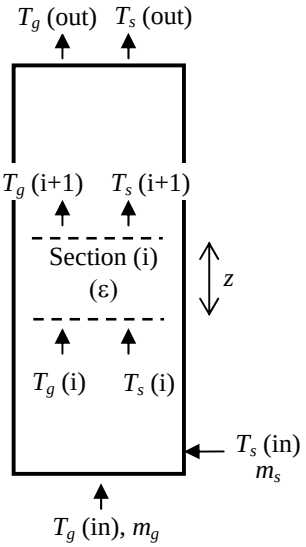

Figure 3. Data analysis method

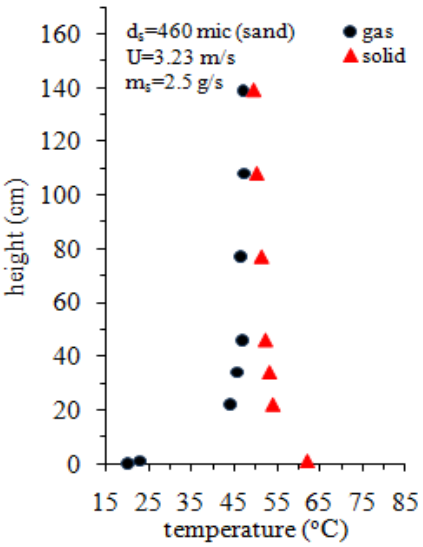

Figure 4. Gas and particle temperature along the CFB riser. Inlet particle temp=70 °C, inlet gas temp=18 °C

RESULTS AND DISCUSSION

Variation of Temperature, Pressure and Particle Concentration

Examples of the variations in the temperature, pressure and particle concentration along the CFB riser are shown in Figs. 4 and 5. These figures typically demonstrate the great complexity and vast variations in the hydrodynamics and heat transfer in such system. The temperature profiles shown in Fig. 4 indicate steep variations at the bottom part of the riser, within the range of ~40 cm above the particle entrance (thermal entrance length). It is interesting to note that both phases are at thermal equilibrium at the height of ~140 cm, just few centimeters below the riser exist. However, for higher particle temperature and particle loading, thermal equilibrium at exit was never reached. This is expected for such a relatively short riser. The pressure and particle volume fraction along the riser are shown in Fig. 5. Similarly, the variations are steep at the dense bottom zone. It is also interesting to note the significant entrance effect on particle concentration near the particle feeding point (10 cm from bottom). This is of significant important since most of the heat transfer takes place in this region.

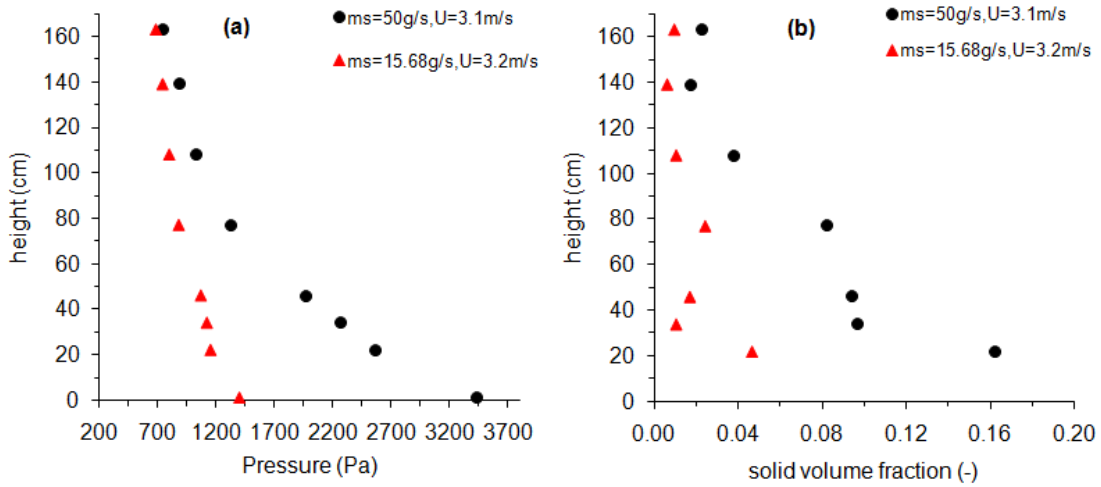

Figure 5. Pressure and particle concentration variations along the riser for glass beads of 700 □m diameter at two different operating conditions.

Particle-Gas Heat Transfer Coefficient

Particle-gas heat transfer coefficient in a dilute CFB is believed to be dominated by particle/gas axial convection. This behavior is rather different than what is observed in CFB boilers and combustors, where the process is controlled by radial convection and conduction between the bed and wall. Therefore, in terms of operating conditions, we are interested in establishing relations between the local heat transfer coefficient and particle/gas axial velocities and particle concentration.

For the range of operating conditions considered in this study the particle-gas heat transfer coefficient was found to fall within the range of 0.1-350. Fig. 6 shows an example of the variations in heat transfer along the riser. As expected, rapid heat transfer takes place at the bottom region, which then decreases towards the top. The thermal entrance length increases with increasing the particle to gas flow ratio. Fig. 7 show the local heat transfer coefficient as function of the particle concentration and axial velocity for data collected from different sections of the riser and at all range of operating conditions considered. The cross-sectional local average particle concentration was obtained from pressure drop measurements (Eq.2) and the average local particle axial velocity was obtained from particle mass flux measurement such that:

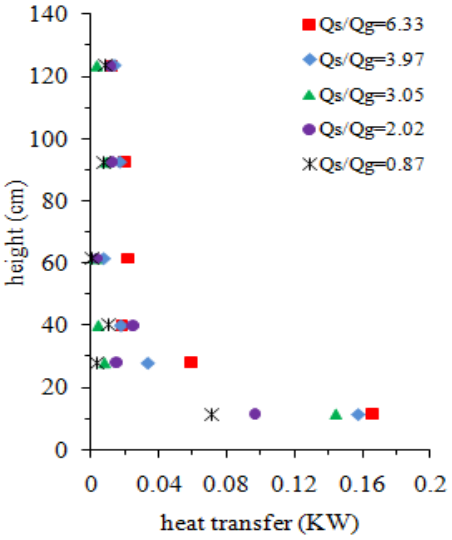

Figure 6. particle-gas heat transfer as function of riser height. Inlet particle temp=70 °C, inlet gas temp= 18 °C

$$u_s = \frac{G_s}{(1-\varepsilon)\rho_s} \tag{10}$$

In Fig. 7a, it is observed that the heat transfer coefficient decreases with increasing particle concentration. This is exactly opposite to CFB wall-bed heat transfer, where the heat transfer coefficient is directly proportional to particle concentration, mainly due to the dominated radial conduction and convection through the dense wall layer. In dilute CFB, the heat transfer mechanism is rather different, dominated by axial convections. As the particle concentration decreases, gas-particle convection diminishes, but at the

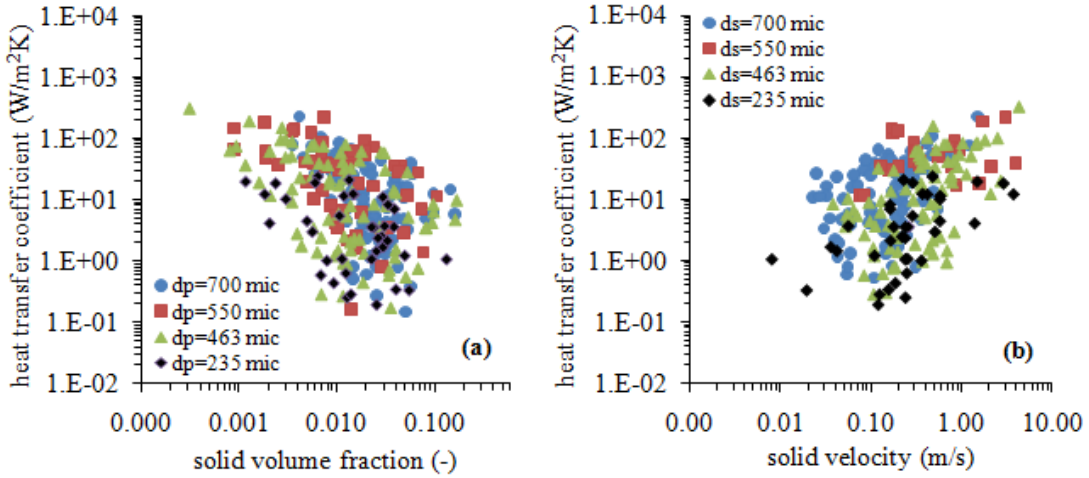

Figure 7. Local heat transfer coefficient as function of particle concentration and velocity

same time the gas convection component becomes important. This is consistent with the observation reported by Rajan et al. (6) and Bandrowski et al. (7), where it is was shown that the heat transfer coefficient decreases with increasing particle concentration within the limit of $\varepsilon > 0.95$. In Fig. 7b the local heat transfer coefficient is observed to consistently increase with increasing the axial particle velocity.

PROPOSED CORRELATION FOR HEAT TRANSFER COEFFICIENT

The analysis shown in section 4.2 suggests that the local particle-gas heat transfer coefficient in the CFB riser can be best correlated with particle velocity, concentration and length of the heat transfer section. Hence, dimensional analysis leads to the following function:

$$h = f\left[\mathrm{Re}_p^{'}, \frac{(1-\varepsilon)z}{d_s}\right] \qquad (11)$$

where the Reynolds number, $\mathrm{Re}_p^{'}$, is expressed in terms of the particle velocity (i.e. $= \rho_g u_s d_s / \mu_g$). Using regression analysis, the following proposed correlation for heat transfer coefficient is obtained:

$$h = 8.4(\mathrm{Re}_p^{'})^{0.871}\left[\frac{(1-\varepsilon)z}{d_s}\right]^{0.924} \qquad (12)$$

This relation is valid for $\varepsilon > 0.8$ and $0.1 < \mathrm{Re}_p^{'} < 200$. Fig. 8 shows the measured heat transfer coefficient for all range of operating conditions considered in the study against the values obtained from Eq. 12.

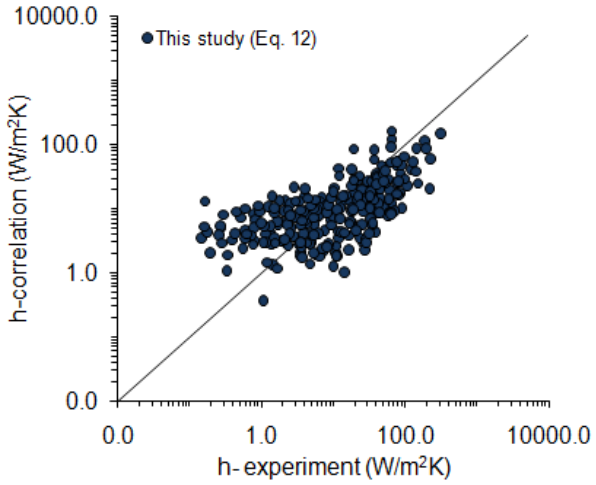

Figure 8. Correlation for heat transfer coefficient

Comparison of the measured heat transfer coefficient and values obtained from literature correlations given in Table 1 is shown in Fig. 9. Generally, the data is scattered; however, Rajan correlation for dense phase (Eq. d) appear to give the closest match with our experimental measurements. The other two

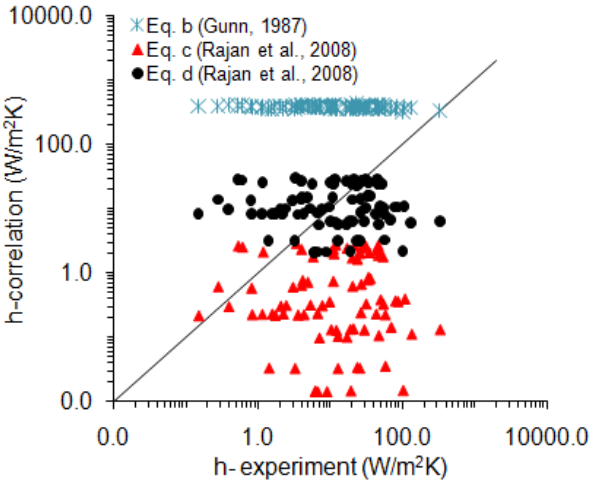

Figure 9. Proposed heat transfer coefficient

correlations, of Gunn (Eq. b) and Rajan for dilute phase (Eq. c), considerably deviates from our measurements. Results from Eq. (a) are omitted as it gives almost the same values as that from Gunn correlation.

CONCLUSION

Particle-gas heat transfer coefficient in a dilute CFB riser ($\varepsilon > 0.8$) has been found to be a strong function of the particle axial velocity, concentration and length of the heat transfer section. A new correlation equation, in terms of these three parameters has been developed. The present experimental data for particle-gas heat transfer coefficient has also been compared with selected correlations from the literature. Work is in progress to extend this correlation to higher temperatures and to incorporate it in *Fluent* CFD code for the simulation of a CFB gasifier.

ACKNOWLEDGEMENT

The author acknowledges the help of Mr. Joseph Eke in the experimental runs.

NOTATION

A_c	cross-sectional area of the riser (m^2)	Re'_p	Reynolds number, = $\rho_g u_s d_s/\mu_g$ (–)
A_s	surface are of particles (m^2)	Re_p	Reynolds number, = $\rho_g U d_s/\mu_g$ (–)
C_p	specific heat capacity (J kg^{-1} K^{-1})	T	temperature (^oC)
d_s	particle diameter (μm)	u	velocity (m s^{-1})
F_e	Fedorov number,$=d_s[4g\rho_g^2(\rho_s/\rho_g-1)/3\mu_g^2]^{0.3}$ (-)	U	superficial gas velocity (m/s)
F_m	particle to gas flow ratio (-)	z	length of heat transfer section (m)
G_s	Particle flux (kg m^{-3} s)		*Greek symbols*
h	particle-gas heat transfer coefficient (W m^{-2} K)	ρ	density (kg m^{-3})
m	mass flow (kg/s)	ε	void fraction (-)
Nu	Nusselt number, $=hd_s/k_g$ (-)		
P	pressure (N m^{-2})		*Subscripts*
Pr	Parndtl number, $=C_p\mu/k_g$ (-)	g	gas
Q	heat transfer (W)	s	particle

REFERENCES

1. Ranz, W. E. Marshall, W. R. (1952). Evaporation from drops, Chem. Eng. Prog. 48 (Part I) (1952) 141–146.
2. Gunn, D. J. (1978). Transfer of Heat or Mass to Particles in Fixed and Fluidised Beds. Int. J. Heat Mass Transfer, 21, 467-476.
3. Xie, D., Bowen, B. D., Grace, J. R., Lim, C. J. (2004). Two-dimensional model of heat transfer in circulating fluidized beds. Part I: Model development and validation, Int. J. of Heat and Mass Transfer 46 (2003) 2179–2191
4. Watanabe, H. Otaka, M. (2006). Numerical simulation of coal gasification in entrained flow coal gasifier, Fuel 85, 1935–1943
5. Fluent 6.3, 1996. Fluent 6.3 Users Guide. Lebanon, NH, 1996, Ansys Inc.
6. Rajan, K. S., Dhasandhan, K., Srivastava, S.N., Pitchumani, B. (2008). Studies on gas–solid heat transfer during pneumatic conveying, Int. J. of Heat and Mass Transfer 51, 2801–2813.
7. Bandrowski, J., Kaczmarzyk, G. (1976). Gas-to-particle heat transfer in vertical pneumatic conveying of granular materials, Chem. Eng. Sci., 1303–1310.